G3, 2025, **15(7)**, jkaf106
https://doi.org/10.1093/g3journal/jkaf106
Advance Access Publication Date: 23 May 2025
Investigation

Large effect life-history genomic regions are associated with functional morphological traits in Atlantic salmon

Tutku Aykanat [1,*], Paul V. Debes [2], Shadi Jansouz,[1] Lison Gueguen,[3] Andrew H. House,[1] Annukka Ruokolainen,[1] Jaakko Erkinaro [4], Victoria L. Pritchard,[5] Craig R. Primmer [1], Geir H. Bolstad [6]

[1]Organismal and Evolutionary Biology Research Program, Faculty of Biological and Environmental Sciences, University of Helsinki, Helsinki 00014, Finland
[2]Department of Aquaculture and Fish Biology, Hólar University, Sauðárkrókur 550, Iceland
[3]Oniris Graduate School of Veterinary Medicine, Nantes 44300, France
[4]Natural Resources Institute Finland (Luke), Oulu 90014, Finland
[5]Institute for Biodiversity & Freshwater Conservation, UHI Inverness, Inverness IV2 5NA, UK
[6]Division of Water and Biodiversity, Norwegian Institute for Nature Research (NINA), Trondheim NO-7485, Norway

*Corresponding author: Organismal and Evolutionary Biology Research Program, Faculty of Biological and Environmental Sciences, University of Helsinki, PO Box 56, Helsinki 00014, Finland. Email: tutku.aykanat@helsinki.fi

Understanding pleiotropic architectures of phenotypes is instrumental for identifying the functional basis of adaptive genetic variation in the wild. Life-history variation may have a morphological basis that mediates resource acquisition allocation pathways, but identifying the underlying genetic basis of such traits is challenging. Using Atlantic salmon (*Salmo salar*) juveniles reared in common garden conditions, we test if 2 life-history associated loci, *six6* and *vgll3*, are also associated with functional morphological traits. These loci had previously shown to exhibit strong signals of adaptation and are highly correlated with sea age at maturity. We show that genetic variation at the *vgll3* locus is linked to variation in morphological traits that underlie swimming performance, along a tradeoff axis between efficient cruising and maneuvering, while the genetic variation at the *six6* locus was linked to variation in body-head proportions suggesting the potential functional importance of these traits for resource acquisition efficiency. However, the direction of changes in morphological traits associated with late- vs early maturing alleles was not always consistent with the expected direction of an effect to maturation timing. Our results reveal a complex morphological landscape associated with the genetic variation in these loci, possibly as a result of pleiotropy or linkage across these genomic regions.

Keywords: Atlantic salmon; morphology; morphometrics; adaptive genetic variation; age at maturity; pleiotropy; *six6*; *vgll3*

Introduction

Elucidating the genotype-phenotype relationship is instrumental in identifying the functional basis of adaptation and the potential targets of selection (Wagner and Altenberg 1996; Kawecki and Ebert 2004; Nielsen *et al.* 2009; Barrett and Hoekstra 2011). Methodological and statistical advances in genetics now allow the identification of genomic regions responding to local selection, but the phenotypic link between genotype and fitness is often missing. Furthermore, many genomic regions can affect a multitude of phenotypic traits (via pleiotropy or linkage disequilibrium), which makes identifying the phenotypic traits under selection even more challenging (Paaby and Rockman 2013; Solovieff *et al.* 2013). Even large-scale genome-wide association studies might be underpowered to detect pleiotropy (Wagner and Zhang 2011). Due to such methodological biased the adaptive significance of pleiotropy can be overlooked especially in natural, non-model populations. However pleiotropy may have substantial effects to limit or promote adaptation (Orr 2000; Otto 2004). In natural systems, pleiotropy has been mostly studied at the phenotypic level to understand the evolutionary tradeoffs by quantifying the physiological antagonisms between senescence and reproduction age. Yet, some studies identify pleiotropic effects of genes associated with adaptive genetic variation. For example, adaptive divergence between lake vs marine morphs of threespine stickleback (*Gasterosteus aculeatus*) was explained by both pleiotropy in the *Eda* gene and via strong linkage with the surrounding loci (Archambeault *et al.* 2020), illustrating the significance of such genetic architectures for adaptation.

Genomic regions with substantial adaptive importance are more likely to be detected in genome scans and are likely to have broad cellular and phenotypic effects (Shapiro *et al.*, 2004; Jones *et al.* 2012; Barson *et al.* 2015). Major effect loci may also have broad cellular and phenotypic effects, with key regulatory roles across development, and could thereby drive strong genetic interdependences among traits (Colosimo *et al.* 2005; Chan *et al.* 2010; Jimenez-Gomez *et al.* 2010; Weith *et al.* 2023) but see (Boyle *et al.* 2017; Jakobson and Jarosz 2020). Therefore, loci exhibiting strong signals of adaptation may provide feasible empirical approaches to understand the significance of complex evolutionary processes, such as how pleiotropy and genetic interactions may hinder or promote adaptation in relation to the direction of natural selection between co-varying traits. Yet, such examples remain rare in non-model, wild organisms (Endler 2000; Mackay *et al.* 2009; Olson-Manning *et al.* 2012; Archambeault *et al.* 2020).

Received on 11 February 2025; accepted on 02 May 2025
© The Author(s) 2025. Published by Oxford University Press on behalf of The Genetics Society of America.
This is an Open Access article distributed under the terms of the Creative Commons Attribution License (https://creativecommons.org/licenses/by/4.0/), which permits unrestricted reuse, distribution, and reproduction in any medium, provided the original work is properly cited.

Downloaded from https://academic.oup.com/g3journal/article/15/7/jkaf106/8142704 by Finnish Forest Research Institute / Library user on 16 December 2025

Functional variation in morphological traits is integral in shaping resource use, and is correspondingly associated with life-history variation and ecotypic divergence in a large array of fish species, including salmonid fishes (Taylor and McPhail 1985; Webb 1988; Ferry-Graham et al. 2002; Svanbäck and Eklöv 2003; Proulx and Magnan 2004; Keeley et al. 2005; Varian and Nichols 2010; Lundsgaard-Hansen et al. 2013; Mindel et al. 2016; Fitzgerald et al. 2017). For example, a fusiform body and shorter fins appear to be advantageous for a long-distance migratory strategy, likely because this body shape reduces the drag (hence the energy consumed) during migration (Morinville and Rasmussen 2007). Likewise, a robust body shape with a larger head, caudal peduncle, and paired fins has been associated with piscivory in rainbow trout (*Oncorhynchus mykiss*, Keeley et al. 2005). Recent population genomics studies in Atlantic salmon have consistently identified 2 unlinked genomic regions, surrounding the genes *six6* in chromosome 9 and *vgll3* in chromosome 25 as strong targets for local selection within all European Atlantic salmon lineages (Barson et al. 2015; Pritchard et al. 2018; Zueva et al. 2020; Miettinen et al. 2023). These 2 loci have also been linked to a suite of life-history traits that strongly influence fitness. In particular, the *vgll3* and *six6* loci are strongly associated with sea age at first maturity (age at maturity from here on) in sea-going salmon at the individual- and population-levels, respectively (Barson et al. 2015, see also, Ayllon et al. 2015 ; Sinclair-Waters et al. 2020), and the *vgll3* locus affects other alternative life-history strategies, such as precocious male maturation (Debes et al. 2021), and iteroparity (Aykanat et al. 2019). For example, individuals with late maturation genotype in the *vgll3* gene ($vgll3^{LL}$) tended to stay at sea, on average, more than 1 year more than individuals with early maturation ($vgll3^{EE}$) genotype (Barson et al. 2015 , Mobley et al. 2021). This pattern was also pertinent during the freshwater phase within which juvenile males with $vgll3^{LL}$ genotype matured at a much higher probability (~60%) than juvenile males with $vgll3^{LL}$ genotype (Debes et al. 2021).

Similarly, these loci explain variation across a number of metabolic and behavioral traits. For example, $vgll3^{E}$ allele has been shown to be associated with reduced aggression, increased maximum metabolic rate (MMR) and aerobic scope (AS) at the juvenile stage (Bangura et al. 2022; Prokkola et al. 2022), while *six6* locus predicts diet acquisition patterns at sea in maturing adults with $six6^{E}$ allele linked to increased stomach weight despite decreased foraging efforts (Aykanat et al. 2020). Likewise, *six6* locus exhibits epistasis with *vgll3* to affect AS variation (Prokkola et al. 2022). The strong genetic interdependence of these phenotypic traits across 2 loci points to the potential for a shared developmental origin (of phenotypes to the respective loci), which is supported by the role of *vgll3* and *six6* in the hormonal and cell fate commitment gene-expression pathways (Kurko et al. 2020; Verta et al. 2020 , 2024; Ahi et al. 2022) and broad expression of *six6* during early development (Moustakas-Verho et al. 2020). Finally, a recent study showed both loci are linked to early life survival in juvenile Atlantic salmon, albeit via parental genetic effects, further supporting broad functional roles across life stages (Aykanat et al. 2024). This collective evidence indicates that these loci are broad-scale modulators of salmon phenotype. While many of these genetic effects have been demonstrated for traits at the juvenile stage, including early male maturation, metabolism, and behavior, any concordance with morphological variation, if any, is not known, but may be important to identify the architecture of personality traits, underlying genetic basis, and evolutionary constrains (Kern et al. 2016 ; Bangura et al. 2022).

To characterize the morphological variation associated with these locally adaptive genomic regions, we collected morphometric data from more than 700 juvenile immature Atlantic salmon at time when male parr maturation may take place (Debes et al. 2021). The fish was reared in common garden conditions and the association between morphology, and *six6* and *vgll3* genotype was estimated with a mixed-effect model that also controls for confounding length and condition factor effects. We identified a suite of morphological characters correlated to the genetic variation in both loci. Our study extends the broad pleiotropic effect of *vgll3* and *six6* loci to functional morphological traits, including phenotypes that are likely important targets of natural selection.

Materials and methods

Fish breeding, and rearing and common garden conditions

Details of the breeding and rearing of individuals from the same cohort were provided in Debes et al (2021), using a similar experimental procedure and facilities, except that the fish in the present study were reared in approximately 2°C cooler water temperature (see, Debes et al (2019) for the details of the rearing temperature). Briefly, the parents of the individuals used were Baltic lineage Atlantic salmon from a broodstock maintained by the Natural Resources Institute Finland (Laukaa, Finland) that were initially originated from the Neva River in Russia (Gulf of Finland in the Eastern Baltic Sea) and has been used for juvenile salmon supplementation in the Kymi river in South-Eastern Finland (Asheim et al. 2023). Parents were crossed using a biallelic cross design where 44 parents were crossed in a 11 two-by-two factorials design. Each factorial unit composed of two males and females. Whereby one in each sex is homozygote for the early (E) maturing allele, and the other for late (L) maturing allele in the *vgll3* locus (i.e. $vgll3^{EE}$ and $vgll3^{LL}$ genotypes, Supplementary Table 1). Therefore, 1 type of genotype within each of the full-sib families were obtained within a two-by-two factorials design, with EE, EL, LE, and LL genotypes in the *vgll3* locus (Supplementary Table 1). *Six6* genotype distribution was not considered during the breeding design, but was segregating in a number of families (Supplementary Table 1). Crosses were performed in November 2017, and offspring were reared in the University of Helsinki fish facilities, first in replicated family-specific compartments in vertical incubators until the swim-up stage. Subsequently offspring of all families were mixed in 8 tanks with roughly balanced proportions of families per tank (Supplementary Table 2). In August 2018, fish were pit-tagged when and fin-clipped for later genotyping. Genotyping and genotypic sex of the parent and offspring were performed by genotyping-by-sequencing using 177 nucleotide polymorphisms (SNPs) which included *vgll3* and *six6* SNPs. The same SNP set were also used for parentage assignment (see, Debes et al. 2021, for details). The rearing temperature of the fish in this study followed a seasonal cycle (range: 4.1–16.0°C) and the natural light regime of the latitude (61.054° N) as described in Debes et al (2019) . In August 2018, the fish were individually PIT-tagged and a fin clip sample was taken to identify the families via genetic pedigree reconstruction. Fish were fed ad libitum except for a short period of restricted feeding for half of the tanks, which included ad libitum feeding for 2 days and then no feeding for 5 days each week for a 5-week period (Debes et al. 2021).

Landmarking and trait measurements

Morphological data were collected as part of a larger effort in December 2018. Fish of both sexes were euthanized using an overdose of tricaine methanesulphonate bath, and stored briefly on ice until imaging was performed the same day. Each fish was sliced

Downloaded from https://academic.oup.com/g3journal/article/15/7/jkaf106/8142704 by Finnish Forest Research Institute / Library user on 16 December 2025

ventrally to collect data on gonad development for another study. The fish was placed on graphical paper, and the body image was taken using a digital camera (Canon PowerShot S110) mounted on a tripod (Hama Star 61), with aperture-priority exposure at F:8, with autofocus option (Supplementary Fig. 1). Cross-sections were obtained by slicing the fish at the posterior end of the dorsal fin (hereafter termed as large cross-section) and adipose fins (hereafter termed as small cross-section), respectively. These were placed on transparent sheets and digitized using a scanner (Epson XP-305) with a modified lid to accommodate the depth of the cross-sections (Supplementary Fig. 1).

Landmarks were placed on the whole body and the 2 cross-sections in a randomized order using imglab software (King 2009), by 2 of the co-authors (LG for landmarked body planes, and SC for landmarked cross-sections) who were blind to any information related to the genotypes or sex of the fish (Supplementary Fig. 2). Landmarks were not placed around the gut region due to the previous ventral slicing. Some landmarks were solely used in the Procrustes analysis to quantify shape, while others were used to quantify specific trait values by calculating the distance between landmarks (Supplementary Fig. 2, Table 1). Traits that were measured twice along the transverse plane (both the left and right sides, Table 1) were averaged prior to analysis. All measurements were reported in centimeters (cm).

Data filtering

At the time of sampling, fish exhibited a bimodal length distribution which is often observed within juvenile salmon from the same cohort (Hoar 1988). Also, a majority of fish used in the analysis (i.e. upper mode of size distribution, see below) had a complete smolt appearance (base on the disappearance of parr marks in the skin and silvery coloration, e.g. Debes *et al.* 2020), or were at late stages of smoltification (faint parr marks with close to silvery skin coloration). We excluded a small number of fish in the lower mode to avoid potential interactions associated with this size bimodality (fish fork length < 9 cm, $N = 69$, Supplementary Fig. 3). In addition, fish with missing *vgll3* and *six6* genotypes, and sex ($N = 2$, $N = 12$, and $N = 4$, respectively), and a small number of precociously matured males ($N = 19$) were excluded from the analysis. Missing landmarks (0.02% of the total landmarks) were imputed using the *estimate.missing* function in the *geomorph* package (version 4.0.6, Baken *et al.* 2021). A landmarked image was excluded from the analysis if more than 1 landmark was identified as an outlier in the Procrustes analysis (i.e. > 4 SD away from the mean). These landmarks were not corrected manually, to avoid introducing among technician variation. After data filtering, 821 individuals remained in the dataset, of which 731, 737, and 772 individuals were in the small cross section, large cross section, and whole body datasets, respectively (Supplementary Table 1). Within each dataset 16, 18, and 712 individuals were landmarked more than once to estimate repeatability. Landmarking for the first 30 and 50 images per researcher for body and cross-sections, respectively, were discarded as training sets.

Trait measurements

We quantified variation in 21 traits across various body planes with potential functional significance using the landmark positions (Supplementary Fig. 2) and as formulated in Table 1.

Rayed fins and caudal peduncle length

We measured the length of dorsal, anal, and tail fins, between interior and exterior insertion points, as well as the caudal peduncle (Table 1, Supplementary Fig. 2). The variation in these traits may be associated with habitat use, feeding, and swimming performance in salmonids and other fishes (e.g. Keeley *et al.* 2005; Jonsson and Jonsson 2011). Increased dorsal and pectoral fin sizes in fish are likely important for increased maneuverability and stability, and likely important adaptations for faster flowing streams (Webb 1984). Specifically, large paired fins (such as pectoral and pelvic fins) in Atlantic salmon are associated with populations that occupy faster flowing and colder streams than slower flowing and warmer rivers, an adaptation attributed to providing effective stability under fast flowing, and turbulent currents (Riddell and Leggett 1981; Webb 1988). In coho salmon, juveniles of interior populations with longer migration distances appear to have smaller fins (Taylor and McPhail 1985), which may help to reduce drag in long migrations (Varian and Nichols 2010).

Eye diameter and position, and snout length

The size of the eye was approximated from the diameter, and the snout length was measured as the distance between the center of the eye and the anterior extreme of the head (Table 1, Supplementary Fig. 2). These traits are morphological features associated with trophic specialization and habitat use across fish taxa (Snorrason 1994; Elmer *et al.* 2010; Peris Tamayo *et al.* 2020).

Aerobic muscle

We approximate the area of aerobic muscle fibers (also called slow-twitch muscle, or red muscle) by measuring the landmark distances in the cross-sections from the lateral line toward the transverse sections, and by measuring the extent of the red muscle along the lateral line (Table 1, Supplementary Fig. 2). Aerobic muscle provides the energy required during steady, cruise swimming and helps with thermal acclimation in fishes (Altringham and Ellerby 1999; Shuman and Coughlin 2018). Recently, it has been shown that both *vgll3* and *six6* loci are associated with whole-body aerobic activity (Prokkola *et al.* 2022), which is a critical physiological process in the salmonid life cycle (Eliason and Farrell 2015), which may indicate that aerobic muscle mass, as a proxy for aerobic activity, may be associated with these loci.

Cross-sectional centroid size and diameter, and vertebral thickness

We measured cross-sectional centroid size and horizontal diameter from both large and small cross-section images (Table 1, Supplementary Fig. 2), as an approximation for fusiform body shape. A slimmer and more torpedo-shaped body provides improved energy efficiency during cruising and in high-flow streams by reducing water drag, and it is an important life history adaptation among fishes (Taylor and McPhail 1985; Webb 1988; Crossin *et al.* 2004; Jonsson and Jonsson 2011). In contrast, a robust cross-section facilitates burst swimming, which is advantageous for prey avoidance and food acquisition (Taylor and McPhail 1985).

We also quantified vertebral width as a proxy for cone diameter to approximate vertebra's flexibility/stiffness during the lateral bending movement in the undulated motion, which helps to maintain steady swimming at the expense of maneuvering capabilities (Long and Nipper 1996; Donatelli *et al.* 2021; Baxter *et al.* 2022).

Head and body size

We quantified head length and width (Table 1, Supplementary Fig. 2), which are important determinants of ecotypic divergence via resource and habitat use in fishes (Simonsen *et al.* 2017; Peris Tamayo *et al.* 2020). A larger head and larger snout length may be associated with a feeding regime toward piscivory (Keeley *et al.* 2005), or generally speaking, consuming larger prey items. We also measured

Downloaded from https://academic.oup.com/g3journal/article/15/7/jkaf106/8142704 by Finnish Forest Research Institute / Library user on 16 December 2025

head and body centroid sizes as an approximation for the area of the morphometric planes, which is the square root of the sum of squared distances of all the landmarks used in the Procrustes analysis from the point of center of gravity (Klingenberg 2016). The Atlantic salmon has a smaller head-body ratio compared with the brown trout (Jonsson and Jonsson 2011), which likely makes salmon more efficient swimmers both in strong freshwater currents and during longer marine migrations.

Statistical analysis

Our analysis framework comprised a series of analyses whereby Procrustes shape variables, and morphological traits were used as response variables. These analyses were conducted independently for the body, small cross-section, and large cross-section. In all analyses, length (centered to zero and scaled to have unit standard deviation), body condition (Fulton's condition factor, scaled), sex, and food treatment were used as covariates. In all models, we implemented genetic variation as additive, where *vgll3* and *six6* genetic effects are coded as 0, 1, and 2 for EE, EL, and LL genotypes, respectively (E and L refer to the alleles associated with early and late maturation, respectively), so that a unit change in genetic effect represents an additive allelic substitution effect from E to L. Unless otherwise noted, all statistical analyses were performed in R software version 4.4.1 (R Core Team 2019).

We performed multivariate generalized Procrustes analysis to quantify shape variation (Gower 1975) using the default settings in the *gpagen* function in the geomorph package (version 4.0.8, Baken *et al.* 2021). This function outputs Procrustes shape variables, centered on the mean value for each landmark and normalized for centroid size. Centroid size is the square root of the sum of squared distances of landmarks from the center of gravity (i.e. centroid) and it is highly correlated to the size of the fish.

Procrustes shape data was then used to perform a Procrustes linear regression analysis using the *procD.lm* function with default settings (i.e. residual randomization was used for significance testing and type III marginal sums of squares for cross-products computations). The model parameters were as follows:

$$Y = \mu + L + CF + Feed + Tank + Sex + Vgll3 + Six6 + Fam + \epsilon_{error}$$

Where Y is the multivariate data frame consisting of *x* and *y* coordinates for Procrustes shape coordinates of landmarks, μ is the intercept, L is the scaled fork length, CF is the scaled Fulton's condition factor, and Feed is the factor associated with feed treatment (ad libitum vs restricted feed). Other terms are the rearing tank ID that the fish were reared after the swim-up stage (Tank), sex (Sex), family (Fam), and the additive genetic effects for *vgll3* (Vgll3) and *six6* (Six6). Since the *procD.lm* function does not accommodate random terms, we included tank and family effects as fixed terms. Trait values were averaged prior to the analyses when an individual had replicate measurements. We reported multivariate analysis of variance Pillai's trace statistics, estimated using the *manova.update* function in the RRPP package (version 2.0.3, Collyer *et al.* 2018), and plot individual landmark differences between loci using the *plotRefToTarget* in the geomorph package.

To decompose the variation associated with trait values and estimate parameter coefficients, we employed a linear mixed-effect (animal) model using the *relmatLmer* function in lme4qtl (version 0.2.2, Ziyatdinov *et al.* 2018), which is an implementation of the *lmer* function in the lme4 package (Bates *et al.* 2015), and can fit the animal model (i.e. accommodate the additive relatedness matrix). When estimating fixed coefficients, the model was fitted with maximum likelihood using the *REML = FALSE* option in the *relmatLmer* function. The model structure was as follows:

$$Y = \mu + L + CF + Feed + Sex + Vgll3 + Six6 + \epsilon_{ID} + \epsilon_{tank} + \epsilon_{animal} + \epsilon_{error}$$

Fixed effect terms are as described above except that the fixed tank and family terms in the previous model were replaced with random tank and animal terms, respectively. Random terms thus included, ϵ_{ID} which are the individual effects, ϵ_{tank} are the effects associated with the tank effects, and ϵ_{error} is the measurement error. ϵ_{animal} is the random term associated with the background genetic effects after controlling for *vgll3* and *six6* fixed effects. The relatedness matrix was obtained using the pedigree data in Debes *et al* (2019) using the *getA* function in the pedigreem package (version 0.3.4, Vazquez *et al.* 2010). Since we used repeated measurements in the analysis, ϵ_{ID} reflects the error term, and ϵ_{error} is the residuals that quantifies deviations between repeated samples (i.e. measurement error).

The significance of the fixed effects terms was estimated using the *as_lmerModLmerTest* function in the lmerTest package (version 1.1-3, Kuznetsova *et al.* 2017) in R using type 3 F test with Satterthwaite's method to estimate the effective degrees of freedom.

We then estimated the additive genetic variation, the contribution of *vgll3* and *six6* loci to the additive genetic variation, evolvability, and repeatability. For these, we employed 3 models similar to above, but the first model ($Model_{VA.full}$) did not contain *vgll3* and *six6* to estimate total additive genetic variation, and was fitted using the *REML = TRUE* option in the *relmatLmer* function to obtain unbiased estimates of variance components. As such, the variance of ϵ_{animal} (V_{animal}) in the $Model_{VA.full}$ is the total additive genetic variation (V_A). Percent contribution of *vgll3* and *six6* are calculated as $\%V_{A.vgll3} = 100 * [(2 \times L_{vgll3} \times E_{vgll3} \times (\beta_{vgll3}{}^2 — se(\beta)_{vgll3}{}^2)/V_{animal}]$, and $\%V_{A.six6} = 100 * [(2 \times L_{six6} \times E_{six6} \times (\beta_{six6}{}^2 — se(\beta)_{six6}{}^2)))/V_{animal}]$, as in (Luo *et al.* 2003), where L_{vgll3}, E_{vgll3}, L_{six6}, and E_{six6} denote frequency of L and E alleles in *vgll3* and *six6* loci, respectively, β_{vgll3} and β_{six6} denote *six6* and *vgll3* E to L substitution effects, respectively, and se denotes standard error of the estimate. Percent repeatability for each model is calculated as $R = V_{ID}/(V_{ID} + V_{error}) * 100$, and heritability values were calculated as $h^2 = V_{animal}/(V_{animal} + V_{tank} + V_{ID})$, where V_{tank}, V_{ID}, and V_{error} are the model variance estimates associated with tank (ϵ_{tank}), individual (ϵ_{ID}), and error (ϵ_{error}) terms in $Model_{VA.full}$. Similarly, evolvability (I_A) was calculated as $V_A/\bar{y}^2$ using $Model_{VA.full}$, where $\bar{y}$ is the mean trait value (Houle 1992; Hansen *et al.* 2011). Evolvabilities are interpreted as expected proportional responses in the trait mean under unit selection (i.e. the selection on fitness itself; Hansen *et al.* 2003; Hansen *et al.* 2011). For all variance components, 95% confidence intervals were estimated by obtaining the posterior distributions of random effect terms in the model ($Model_{VA.full}$), using the *sims* function in the arm package(version 1.1.4-4, Gelman and Su, 2020) in R, using 10,000 permutations. The simulations generate 10,000 estimates for random effect terms, which are then used to calculate the variance components as above, with 250th and 9750th ranked estimates recorded as 95% CIs. We did not control for the effect of dominance in the analyses, which may have inflated the estimates of additive genetic variance (Lynch and Walsh 1998).

Results

Shape analysis

The multivariate analyses using Procrustes shape variation as the response showed that genetic variation in *six6*, but not in *vgll3*, is

Downloaded from https://academic.oup.com/g3journal/article/15/7/jkaf106/8142704 by Finnish Forest Research Institute / Library user on 16 December 2025

Table 1. Estimated fixed effect coefficients for 21 morphological traits obtained across 3 body planes.

Trait	Body Plane[c]	Trait value formula[c]	Intercept	Length (scaled)		Condition factor (scaled)		Feed restriction (ad libitum to restricted)		Sex (female to male)		vgll3 (E to L)		six6 (E to L)	
			coef. (SE)	coef. (SE)	*P*-value	coef. (SE)	*P*-value	coef. (SE)	*P*-value	coef. (SE)	*P*-value	coef. (SE)	*P*-value	coef. (SE)	*P*-value
Dorsal fin	B	B [12:13]	2.0439 (0.0305)	0.1560 (0.0064)	<0.001[b]	−0.0016 (0.0041)	0.696	−0.1222 (0.0176)	<0.001[b]	0.0228 (0.0124)	0.067	−0.0246 (0.0148)	0.106	−0.0142 (0.0126)	0.263
Anal fin	B	B [16:17]	1.35902 (0.0164)	0.06636 (0.0041)	<0.001[b]	0.00043 (0.0038)	0.909	−0.02549 (0.0094)	0.0402[a]	0.01759 (0.0076)	0.021[a]	−0.01979 (0.0077)	0.017[a]	0.00658 (0.0075)	0.378
Pectoral fin	B	B [10:11]	2.0973 (0.0202)	0.1148 (0.0029)	<0.001[b]	0.0082 (0.0022)	<0.001[b]	−0.0376 (0.0151)	0.059	0.0143 (0.0053)	0.007[b]	−0.0102 (0.0096)	0.29	0.0030 (0.0058)	0.601
Tail fin	B	B [19:20]	8.3e-01 (0.0098)	4.1e-02 (0.0015)	<0.001[b]	−8.2e-03 (0.0013)	<0.001[b]	−2.1e-02 (0.0037)	0.003[b]	2.8e-05 (0.0027)	0.992	−4.0e-03 (0.0051)	0.432	3.1e-03 (0.0030)	0.292
Caudal peduncle	B	B [15:18]	8.7e-01 (0.00428)	6.0e-02 (0.00078)	<0.001[b]	1.1e-02 (0.00071)	<0.001[b]	1.3e-03 (0.00198)	0.529	2.3e-03 (0.00144)	0.118	−2.3e-03 (0.00219)	0.294	−6.7e-05 (0.00153)	0.965
Vertebra thickness	Sml	S [3:4]	2.4e-01 (0.00265)	1.6e-02 (0.00081)	<0.001[b]	1.8e-03 (0.00082)	0.0241[a]	2.3e-03 (0.00165)	0.172	−2.2e-03 (0.00157)	0.168	−3.3e-03 (0.00117)	0.009[b]	5.3e-05 (0.00138)	0.969
Vertebra thickness	Lrg	L [6:7]	0.25170 (0.00282)	0.01394 (0.00077)	<0.001[b]	0.00467 (0.00078)	<0.001[b]	−0.00238 (0.00155)	0.125	−0.00244 (0.00146)	0.096	−0.00297 (0.00131)	0.032[a]	0.00023 (0.00137)	0.866
Cross-section diameter	Sml	S [5:7]	1.1423 (0.0136)	0.0753 (0.0027)	<0.001[b]	0.0134 (0.0027)	<0.001[b]	−0.0562 (0.0114)	0.003[b]	0.0020 (0.0049)	0.683	−0.0157 (0.0058)	0.012[a]	−0.0054 (0.0050)	0.279
Cross-section diameter	Lrg	L [12:8]	2.0269 (0.0117)	0.1477 (0.0021)	<0.001[b]	0.0312 (0.0021)	<0.001[b]	0.0050 (0.0108)	0.666	0.0019 (0.0039)	0.621	−0.0047 (0.0048)	0.335	−0.0046 (0.0039)	0.248
Aerobic muscle	Sml	S [(7:8 + 5:6)/2]	0.17549 (0.00353)	0.01024 (0.00082)	<0.001[b]	0.00137 (0.00083)	0.0981	−0.01237 (0.00290)	0.0051[b]	0.00056 (0.00153)	0.715	−0.00557 (0.00148)	<0.001[b]	−0.00210 (0.00149)	0.159
Aerobic muscle	Lrg	L [(8:9 + 12:13)/2)	0.2349 (0.00408)	0.0185 (0.00094)	<0.001[b]	0.0033 (0.00094)	<0.001[b]	0.0070 (0.00239)	0.025[a]	0.0017 (0.00175)	0.34	−0.0024 (0.00195)	0.222	−0.0022 (0.00174)	0.198
Aerobic muscle vertical extension	Lrg	L [(14:15 + 10:11)/2]	0.879 (0.0198)	0.087 (0.0039)	<0.001[b]	0.026 (0.0039)	<0.001[b]	0.038 (0.0176)	0.0916	−0.012 (0.0073)	0.089	−0.024 (0.0081)	0.006[b]	0.013 (0.0072)	0.067
Eye diameter[d]	B	B [(2:3 + 4 + 5)/2]	5.5e-01 (0.00358)	2.2e-02 (0.00094)	<0.001[b]	3.3e-04 (0.00092)	0.723	1.8e-03 (0.00285)	0.546	−1.7e-06 (0.00175)	0.999	−3.2e-03 (0.00152)	0.055	2.6e-03 (0.00163)	0.112
Snout length	B	B [1:0]	0.78061 (0.00458)	0.03839 (0.00097)	<0.001[b]	−0.00054 (0.00083)	0.509	−0.00277 (0.00196)	0.157	0.00557 (0.00183)	0.002[b]	−0.00607 (0.00232)	0.013[a]	0.00575 (0.00189)	0.002[b]
Eye vertical position	B	B [0:6]	0.40996 (0.0052)	0.02487 (0.0012)	<0.001[b]	0.00460 (0.0010)	<0.001[b]	0.00934 (0.0036)	0.0538	0.00024 (0.0022)	0.912	−0.00031 (0.0024)	0.899	0.00057 (0.0022)	0.794
Head length[e]	B	B [1:7]	2.1453 (0.0232)	0.1347 (0.0034)	<0.001[b]	0.0074 (0.0025)	0.0034[a]	−0.0370 (0.0224)	0.162	0.0106 (0.0064)	0.094	−0.0074 (0.0098)	0.455	0.0146 (0.0068)	0.032[a]
Head width[e]	B	B [8:9]	1.59855 (0.0052)	0.09654 (0.0015)	<0.001[b]	0.01633 (0.0013)	<0.001[b]	0.02432 (0.0030)	<0.001[b]	0.00420 (0.0028)	0.13	−0.00046 (0.0024)	0.85	0.00030 (0.0026)	0.907
Body centroid size	B	From Procrustes analysis	13.1556 (0.0201)	0.9084 (0.0031)	<0.001[b]	0.0090 (0.0026)	<0.001[b]	0.0505 (0.0124)	0.0118[a]	−0.0088 (0.0057)	0.124	0.0253 (0.0099)	0.014[a]	−0.0227 (0.0061)	<0.001[b]
Head centroid size	B	From Procrustes analysis	2.2095 (0.0131)	0.1312 (0.0020)	<0.001[b]	0.0143 (0.0016)	<0.001[b]	−0.0073 (0.0144)	0.632	0.0077 (0.0037)	0.040[a]	−0.0075 (0.0050)	0.148	0.0104 (0.0039)	0.008[b]
Centroid size	Sml	From Procrustes analysis	1.4166 (0.0129)	0.0968 (0.0023)	<0.001[b]	0.0199 (0.0023)	<0.001[b]	−0.0387 (0.0102)	0.0111[a]	0.0033 (0.0042)	0.432	−0.0119 (0.0058)	0.048[a]	−0.0048 (0.0044)	0.28
Centroid size	Lrg	From Procrustes analysis	3.5944 (0.0177)	0.2598 (0.0029)	<0.001[b]	0.0601 (0.0029)	<0.001[b]	0.0202 (0.0133)	0.209	−0.0015 (0.0053)	0.778	−0.0097 (0.0082)	0.244	−0.0054 (0.0056)	0.337

Trait lengths are given in centimeters (cm) for all traits. Coef. (SE) indicates coefficients and their standard error. B, S, and L in the body plane column indicates lateral view of the body, small and large cross-sections, respectively.

[a] $P < 0.05$.

[b] $P < 0.01$.

[c] The trait values are based on landmarks as numbered and indicated in Supplementary Fig. 2.

[d] Eye origin is the center point of eye landmarks, and calculated using landmarks 2, 3, 4, and 5, which are the anterior, posterior, dorsal and ventral extremes of the bony orbit of the eye.

[e] Landmark 7 is the posterior point of the bony operculum. Landmarks 8 and 9 are the points of maximum curvature of the bony operculum at the ventral and dorsal ends, respectively.

Downloaded from https://academic.oup.com/g3journal/article/15/7/jkaf106/8142704 by Finnish Forest Research Institute / Library user on 16 December 2025

Table 2. Multivariate analysis using procrustes shape variable across 3 body planes in juvenile Atlantic Salmon.

Terms	Large cross-section				Small cross-section				Body			
	df	Pillai	z-value	P-value	df	Pillai	z-value	P-value	df	Pillai	z-value	P-value
Length (scaled)	1	0.207	8.231	0.001	1	0.042	2.574	0.008	1	0.530	15.369	0.001
Condition factor (scaled)	1	0.053	1.398	0.074	1	0.024	0.894	0.195	1	0.478	10.583	0.001
Feed restriction	1	0.096	3.924	0.001	1	0.102	6.035	0.001	1	0.284	12.050	0.001
Family	37	1.939	9.994	0.001	37	0.721	2.200	0.011	37	2.446	24.524	0.001
Tank	4	0.312	6.244	0.001	4	0.219	7.020	0.001	3	0.276	8.643	0.001
Sex	1	0.035	−0.118	0.548	1	0.013	−0.597	0.717	1	0.038	1.185	0.121
vgll3	1	0.042	0.495	0.318	1	0.018	0.108	0.461	1	0.032	0.562	0.285
six6	1	0.027	−0.992	0.831	1	0.013	−0.617	0.739	1	0.052	2.454	0.013
Full model	47	2.727	14.021	0.001	47	1.256	7.674	0.001	46	3.929	23.997	0.001
Residuals	689				681				724			

Pillai is the Pillai's trace test statistic to evaluate each term's significance in the multivariate analysis of variance.

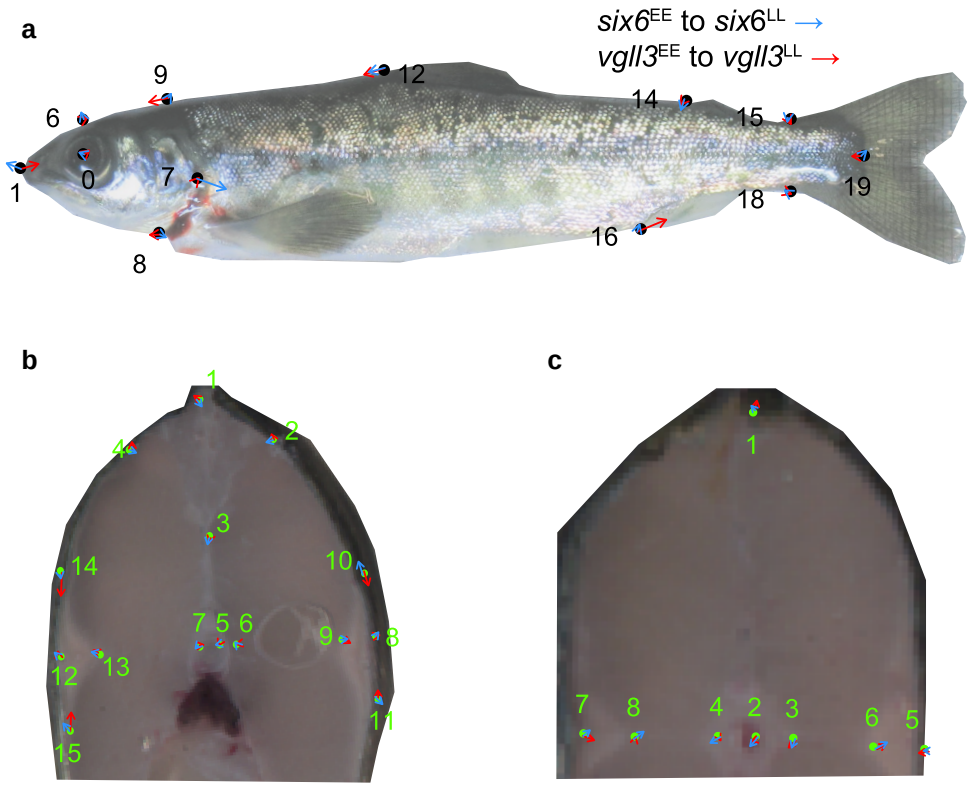

Fig. 1. The difference between $vgll3^{EE}$ and $vgll3^{LL}$ (blue lines), and $six6^{EE}$ and $six6^{LL}$ (red lines) genotypes on body shape of juvenile Atlantic salmon using thin-plate spline in the body a), large cross-section b), and small cross-section c). The black dots in a, and green dots in b and c are the predicted shape coordinate associated with $vgll3^{EE}$ and $six6^{EE}$ after the generalized Procrustes analysis. For all images, the effect sizes are magnified by 10×. Landmark numbers are based on Supplementary Fig. 2. Note that the body and cross-section images are to illustrate the location of landmarks on these body planes, and were slightly distorted to fit onto the average coordinates obtained by Procrustes analysis.

associated with shape change in the body plane (Table 2). The change in the body plane appears to be related to changes in the head region associated with *six6*, whereby a substitution from $six6^{E}$ to $six6^{L}$ elongates the head and slightly bends up the lateral body positioning at ends of the lateral line. In contrast, $vgll3^{E}$ to $vgll3^{L}$ substitution reduces the head area relative to the body area and pushes the anterior anal fin landmark toward the posterior end of the body plane, albeit the effect is statistically insignificant (Fig. 1a). Genetic variation in *vgll3* and *six6* is not associated with overall shape changes in small and large cross-sections. Although not statistically significant, a $vgll3^{E}$ to $vgll3^{L}$ substitution was linked with a narrower horizontal width, a smaller aerobic muscle area in the small cross-section (Fig. 1b), and a narrower aerobic muscle extension perpendicular to the lateral line in the large cross-section (Fig. 1c). These results are concordant with the trait-based analysis (see below). Overall, family, tank, feed restriction, and length were important determinants of shape variation in all planes, and condition factor was also significant in the analysis of the body plane (Table 2). Sex was an insignificant determinant of shape in all 3 body planes (Table 2).

Trait analysis

After correcting for body length, condition factor, feed restriction, and sex, 9 out of 21 morphological traits were significantly associated with the *vgll3* locus, while 4 were associated with *six6* locus (Table 1, Fig. 2. See also Supplementary Table 3 for *t*-values and

Downloaded from https://academic.oup.com/g3journal/article/15/7/jkaf106/8142704 by Finnish Forest Research Institute / Library user on 16 December 2025

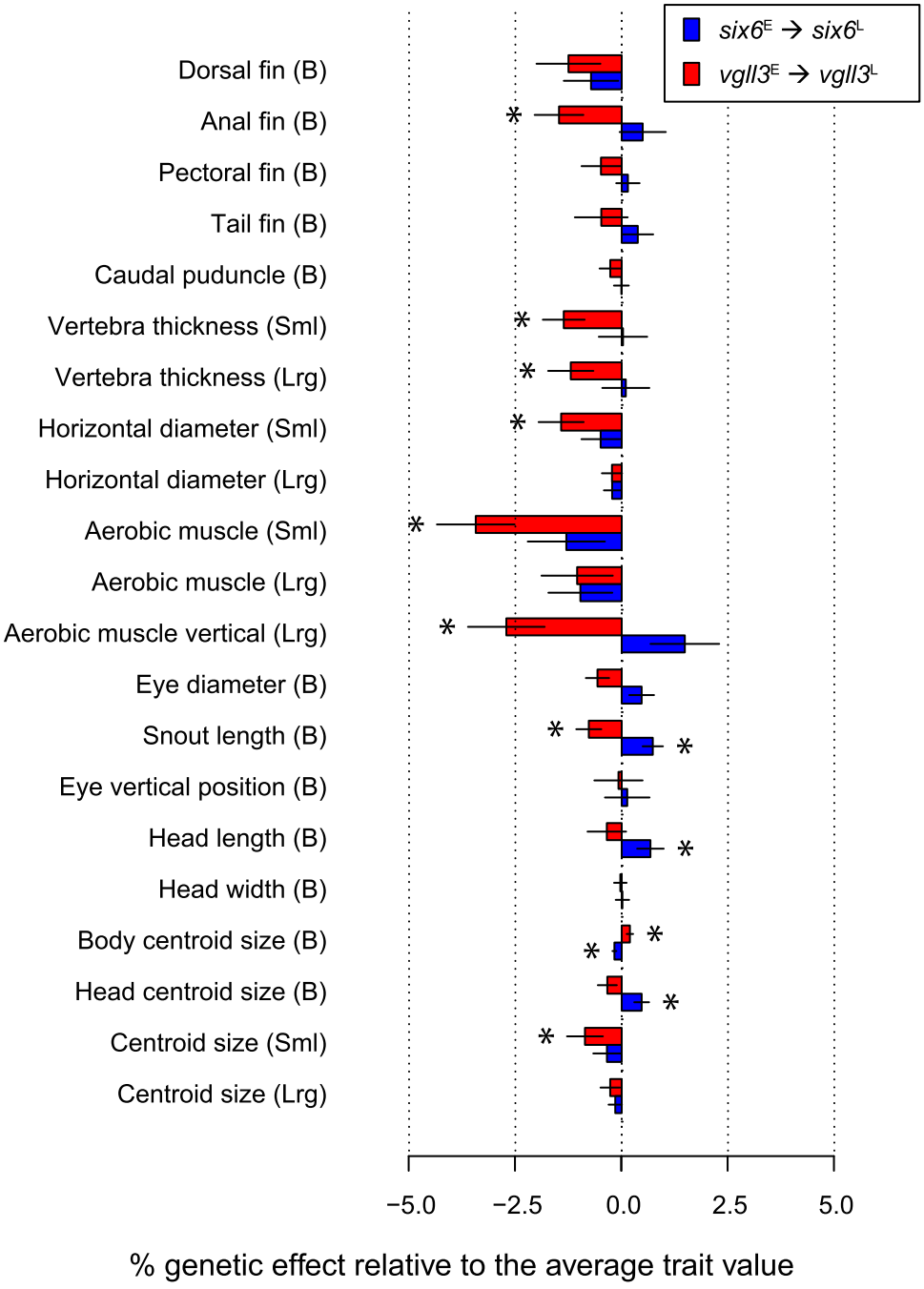

Fig. 2. Percent trait value change associated with *vgll3*^{E} to *vgll3*^{L} (red lines), and *six6*^{E} to *six6*^{L} (blue lines) allelic substitutions relative to the average trait values. Asterisks denote significant genetic effect. Error bars indicate 1 standard error.

effective degrees of freedoms of terms). In general, the *vgll3*^{E} to *vgll3*^{L} substitution effect decreased trait values (Table 1, Fig. 2) with changes in trait values between *vgll3*^{EE} and *vgll3*^{LL} genotypes being > 1%, and up to 3% of the mean trait values (Fig. 2). Notably, the aerobic muscle depth in the small cross-section was reduced by 3.45% ($P < 0.001$) and the aerobic muscle vertical extension in the large cross-section was reduced by 2.72% ($P = 0.006$) by the *vgll3*^{E} to *vgll3*^{L} allelic substitution (Table 1, Fig. 2). The *vgll3* allelic substitution effect associated with lateral red muscle length was statistically significant when 3 aerobic muscles trait values were combined into 1 composite value ($P < 0.001$, Supplementary Table 4). The *vgll3*^{L} allele also decreased vertebral thickness in both small (1.37% decrease, $P = 0.009$) and large (1.21% decrease, $P = 0.032$) cross-sections (Table 1, Fig. 2). The *vgll3*^{E} to *vgll3*^{L} substitution effect significantly reduced the small cross-section diameter by 1.43% ($P = 0.012$), whereas the small section centroid size was reduced by 0.86% ($P = 0.012$, Table 1, Fig. 2). Reduced eye diameter, snout length, and anal fin length were also associated with the *vgll3*^{L} allele (Table 1, Fig. 2). The trait values for all ray fins (dorsal, anal, pectoral, and tail fins) were trending toward a smaller size in relation to the late maturing genotype (Table 1, Fig. 2), and their cumulative effect, i.e. effect size of all trait values combined, was statistically significant ($P = 0.022$, Supplementary Table 4). We observed that in some traits the variation explained by *vgll3*^{E} to *vgll3*^{L} substitution was up to 50% of the variation explained by length (a factor with strong, positive allometric effect

Downloaded from https://academic.oup.com/g3journal/article/15/7/jkaf106/8142704 by Finnish Forest Research Institute / Library user on 16 December 2025

on other trait values, see Table 1), suggesting that this variation is biologically important (Supplementary Fig. 4).

Most differences explained by variation in the *six6* genomic region were related to changes in head and body size. The $six6^{E}$ to $six6^{L}$ substitution was associated with a 0.17% decrease in body centroid ($t = -3.70$, $P < 0.001$) and a 0.47% increase in head centroid size ($t = 2.68$, $P = 0.008$, Table 1, Fig. 2). The snout length, measured as the distance between the center of the eye and the maximum anterior point in the body, was elongated by 0.73% in fish with an additional $six6^{L}$ allele ($t = 3.05$, $P = 0.002$, Table 1, Fig. 2). Head length appears to be a significant determinant of changes in head structure, the effect of an additional $six6^{L}$ allele explained a 0.33% increase in average trait value ($t = 2.15$, $P = 0.032$, Table 1, Fig. 2).

Sex effects typically ranged from smaller up to the same order of magnitude as the allele substitution effects in the life-history loci (Table 1). Notably, the snout, pectoral fin, and anal fin were significantly larger in males compared with females ($P = 0.002$, $P = 0.007$, and $P = 0.021$, respectively Table 1). In addition, the head centroid was larger in males compared with females ($P = 0.040$, Table 1). As expected, length was a strong predictor of all traits, and condition factor was also positively associated with most traits (Table 1). Feed restriction was notably associated with a decrease in fin trait values, such as the dorsal fin ($P < 0.001$), anal fin ($P = 0.040$), and tail fin ($P = 0.003$, Table 1). Interestingly, feed restriction substantially reduced the centroid size ($P = 0.011$), cross-section diameter ($P = 0.003$), and the size of the aerobic muscle ($P = 0.005$) in the small cross-section, but not in the large cross-section (Table 1).

As length is a strong predictor of both trait values and overall body shape, a spurious association between traits and the life-history loci may be expected if these loci affect trait values via length as a mediator. To test this, we constructed a model to include the interaction between length and life-history loci. Across 21 traits, we did not observe a meaningful difference in main genetic effects, nor were interaction term *t*-values substantial (Supplementary Fig. 5), suggesting that length-by-genotype interaction did not drive the estimated relations.

Heritability, evolvability, and additive genetic variation: Trait heritabilities were low to moderate in most cases, with a mean heritability of 0.19 across all 21 traits (Table 3). Length of tail fin and body centroid size exhibited the highest heritability with 0.50 (95% CI 0.47–0.54) and 0.47 (95% CI 0.43–0.50), followed by the pectoral fin with 0.41 (95% CI 0.36–0.45). The repeatability of trait measurements was moderate (mean repeatability 73.0%, Table 3). The relatively low repeatability than expected (Takacs *et al.* 2016) is likely due to low intra-population variation obtained in the common garden setting relative to most morphometrics studies that focuses on larger biological variation, e.g. between ecomorphs of conspecifics or across species, but complex trait measurements combined with suboptimal fish imaging using gutted individuals, and measurer's expertise may also contribute to such variation (Takacs *et al.* 2016; Vrdoljak *et al.* 2020).

Evolvabilities (mean-scaled additive genetic variances, denoted as I_A) differed greatly among traits (Table 3). Interestingly, body centroid size had the lowest evolvability (<0.001), meaning that even under unit directional selection (the strength of selection on fitness itself, Hansen *et al.* 2003), the expected increase in this trait value would be less than 0.1%. On the other hand, large cross-section aerobic muscle had an evolvability as high as 0.72, meaning that the expected increase in this trait under strong selection could be as high as 71% of the mean trait value. In general, out of 21 traits measured, aerobic muscle and vertebrae thickness traits had higher I_A, while centroid sizes and cross-section diameters had lower I_A (Table 3).

Additive genetic variation explained by the *vgll3* locus was nonzero for 12 traits (Table 3). Consistent with the fixed effect parameterization of the genotype, a substantial portion of the additive genetic variation in vertebra thickness was explained by *vgll3*, with 30.7 and 13.0% for small and large cross-sections, respectively (Table 3). A significant portion of the additive genetic variation in small section aerobic muscle, cross-section diameter, and body centroid was also explained by the *vgll3* locus, with 22.4, 12.7, and 6.3% for each trait, respectively (Table 3). Consistent with the locus effect size, the contribution of *six6* locus to additive genetic variation included snout length (9.4%), and head and body centroid size (5.2 and 4.2%, respectively, Table 3).

Discussion

Intraspecific differences in functionally important morphological traits may provide important insights into the mechanistic basis of adaptation. We detected several morphological traits in juvenile Atlantic salmon that were linked with variation in genomic regions previously reported to be associated with life-history diversity and known to be under local selection. The genetic polymorphism in the *vgll3* locus appears to shape a suite of traits associated with swimming performance, while the genetic polymorphism in the *six6* locus shapes head and body size, and head features such as snout length, which potentially affects resource acquisition efficiencies for different foraging strategies. On the other hand, these genomic regions have only a small effect on the general shape of the morphological planes. The only statistically significant effect detected was associated with the *six6* loci in the body plane (Table 2), for which the most striking shape change at the vector level elongates the head length (in relation to $six6^{E}$ to $six6^{L}$ substitution, Fig. 1). This is concordant with change in the head/body proportions observed in the univariate trait analysis. Our results support these genomic regions having broad phenotypic effects, which may have emerged from either a form of pleiotropy or linkage disequilibrium. Our design does not allow us to categorize the pleiotropic effects further, whether it is based on an effect of single causal variant (biological pleiotropy), or based on effects associated with different phenotypes along a biochemical pathway (mediated pleiotropy), or as a result of linkage disequilibrium between 2 independent causative loci (spurious pleiotropy, e.g. Solovieff *et al.* 2013). Yet, the strong genetic interdependence among traits associated with *six6* and *vgll3* may have a developmental origin, which is supported by the patterns of gene expression in these genomic regions during development (Kurko *et al.* 2020; Moustakas-Verho *et al.* 2020), and their molecular regulatory functions, (Kurko *et al.* 2020; Verta *et al.* 2020; Mobley *et al.* 2021; Ahi *et al.* 2022, 2024). For example, being a co-transcription factor binding to the TEAD protein, *vgll3* is likely an important regulator of the hippo pathway (Kurko *et al.* 2020) which is involves in organ growth via controlling cell growth (Huang *et al.* 2005). Likewise, allele specific *vgll3* regulation of pubertal development, interact with signaling pathways with diverse molecular functions, such as TGF- β signaling, and wnt pathway which have developmental functions during body axes formation, as well as cell fate commitment (Wu and Hill 2009; Xue *et al.* 2025).

The suite of morphological traits associated with *vgll3* variation reflects changes along a functional axis that facilitates energy-efficient cruising ($vgll3^{L}$) vs maneuvering and acceleration ($vgll3^{E}$). It appears that that individuals with $vgll3^{E}$ genotype have a robust

Downloaded from https://academic.oup.com/g3journal/article/15/7/jkaf106/8142704 by Finnish Forest Research Institute / Library user on 16 December 2025

Table 3. Variance components for 21 morphological traits obtained from 3 body planes.

Trait[a]	Body Plane[b]	V_A[a]	% $V_{A.vgll3}$	%$V_{A.six6}$	h^2	I_A[c]	% rep.
Dorsal fin	B	0.0032 (0.0027–0.0036)	2.6	0	0.083 (0.072–0.095)	0.045 (0.042–0.048)	95.2
Anal fin	B	7.7e–04 (6.8 e–04–8.8e–04)	17.2	0	0.07 (0.061–0.08)	0.27 (0.26–0.3)	67.3
Pectoral fin	B	0.0027 (0.0024–0.003)	0	0	0.41 (0.36–0.45)	0.016 (0.015–0.017)	83.7
Tail fin	B	8.2e–04 (7.3e–04–9.1e–04)	0	0	0.5 (0.47–0.54)	0.051 (0.048–0.055)	69.7
Caudal peduncle	B	1e–04 (9.1e–05–1.2e–04)	0	0	0.26 (0.24–0.29)	0.02 (0.019–0.021)	65.3
Vertebra thickness	Sml	1.3e–05 (1.1e–05–1.5e–05)	30.7	0	0.039 (0.033–0.045)	0.31 (0.28–0.35)	63.7
Vertebra thickness	Lrg	2.0e–05 (1.7e–05–2.3e–05)	13	0	0.06 (0.052–0.069)	0.21 (0.19–0.23)	71.4
Cross-section diameter	Sml	6.8e–04 (5.9e–04–7.9e–04)	12.7	0	0.12 (0.11–0.14)	0.0099 (0.009–0.011)	97.6
Cross-section diameter	Lrg	3.3e–04 (2.9e–04–3.8 e–04)	0	0	0.11 (0.093–0.12)	0.012 (0.01–0.013)	84.1
Aerobic muscle	Sml	5.8e–05 (5.1e–05–6.7e–05)	22.4	0	0.19 (0.17–0.21)	0.69 (0.62–0.76)	56.5
Aerobic muscle	Lrg	7.5e–05 (6.6e–05–8.7e-05)	0	0	0.37 (0.34–0.41)	0.72 (0.65–0.79)	24.0
Aerobic muscle vertical extension	Lrg	0.001 (8.6 e–04–0.0012)	22.2	2.3	0.1 (0.087–0.12)	0.29 (0.26–0.32)	78.5
Eye diameter	B	3.1e–05 (2.7e–05–3.5e–05)	8.6	1.6	0.11 (0.094–0.12)	0.23 (0.21–0.24)	25.9
Snout length	B	9.0e–5 (7.9e–05, 1e–04)	14.1	9.4	0.12 (0.11–0.14)	0.023 (0.021–0.024)	82.4
Eye vertical position	B	6.4e–05 (5.6e–05–7.3e–05)	0	0	0.06 (0.052–0.069)	0.15 (0.14–0.16)	79.7
Head length	B	0.0022 (0.0019–0.0025)	0	1.8	0.22 (0.19–0.26)	0.018 (0.017–0.02)	88.9
Head width	B	3.5e–05 (3e–05–4e–05)	0	0	0.021 (0.018–0.025)	0.02 (0.019–0.022)	75.4
Body centroid size	B	0.0034 (0.0031–0.0038)	6.3	4.2	0.47 (0.43–0.5)	7.6e-04 (7,1e-04, 8.2e-04)	73.8
Head centroid size	B	5e–04 (4.4e–04–5.7e–04)	0.5	5.1	0.15 (0.12–0.17)	0.009 (0.0084–0.0096)	85.1
Centroid size	Sml	8.3e–04 (7.2e–04–9.5e–04)	4.4	0	0.27 (0.24–0.3)	0.043 (0.039–0.048)	71.5
Centroid size	Lrg	0.0014 (0.0012–0.0016)	0	0	0.22 (0.19–0.24)	0.0025 (0.0023–0.0028)	93.5

V_A, h^2, and I_A are additive genetic variance, heritability, and evolvability, respectively, after controlling for length, condition factor, feed restriction, and sex.% $V_{A.vgll3}$ and%$V_{A.six6}$ are additive genetic variation explained by the *vgll3* and six6 loci, respectively (values are truncated to zero if the estimate is less than zero). Values indicate medians, with 95% CI given in parenthesis. % rep. indicate the percent repeatability estimated from repeated measurements of individuals, and to assess the contribution of measurement error to trait measurements.

[a]Trait length unit is cm for all traits. The unit of V_A is cm^2.

[b]The trait values are based on landmarks as numbered and indicated in Supplementary Fig. 2. B, S, and L prefixes represent body, small cross-section, and large cross-sections, respectively.

[c]I_A is measured as V_A divided by the squared trait mean, and it is units free.

built to facilitate maneuvering and acceleration, and larger aerobic activity (i.e. increased red muscle area, see also below), while individuals with $vgll3^L$ allele have a slender body build for energy efficiency swimming (i.e. smaller cross-section diameter, and smaller ray fins, see also below). Energy efficient cruising is an important trait especially in the marine environment, while better maneuvering and acceleration help coping with biotic (i.e. competition and predation risk) and abiotic (flow regime) factors in the freshwater habitat. The larger aerobic muscle area associated with the $vgll3^E$ allele could indicate a higher potential for aerobic muscle activity. This result is concordant with (Prokkola *et al.* 2022) who demonstrated that juvenile Atlantic salmon with the early maturing genotype have a higher MMR and AS. Aerobic locomotion is expected to be central for Atlantic salmon during the marine phase, where salmon sub-adults migrate and continuously forage for food. Our results suggest salmon with the early genotype are more likely to maintain sustained swimming and foraging activities, beneficial during marine exploration, which may help to facilitate earlier maturation, with poor performers having to delay reproduction until they can utilize sufficient energy for return migration. On the other hand, having a slender body and energy-efficient cruising may be more advantageous in later years, since individuals with more $vgll3^L$ alleles appears to perfrom better than indiviauls with $vgll3^E$ allale at older sea-age groups (i.e. Barson *et al.* 2015). It is unclear if the genetic association between life-history loci and morphological traits persists between life stages, or across different environments. The parr-smolt transformation (smoltification) includes morphological changes that prepare juvenile Atlantic salmon for the marine environment (Jonsson and Jonsson 2011); hence, phenotype-genotype association might differ either as a result of smoltification or change in the environment (Aguirre *et al.* 2014). However, since individuals used in this study have a complete or nearly complete smolt phenotype, conclusions may be more relevant to the marine than to the freshwater life stage.

Increased vertebral thickness associated with the $vgll3^E$ allele could provide stiffness for energy-efficient undulation movement during steady swimming (Donatelli *et al.* 2021), though it may

Downloaded from https://academic.oup.com/g3journal/article/15/7/jkaf106/8142704 by Finnish Forest Research Institute / Library user on 16 December 2025

come at the expense of body flexibility that may facilitate piscivorous prey capture. A larger aerobic muscle area and thicker vertebra may eventually facilitate earlier maturation via more energy efficient resource acquisition at sea, suggesting that local adaptation for optimal age structure could be partly mediated by conditions at sea. Hence, while our results do not explain the causation of early male maturation in freshwater, we cannot explicitly rule out that the link between *vgll3* and age at maturity is mediated via its effect on body shape.

Sex was also an important factor shaping the trait variation. Intriguingly, significant changes in shape associated with sex and *vgll3* genotype were also in concordant with respect to maturation timing. As such, males, which on average mature earlier than females, and the *vgll3* allele associated with early maturation had similar direction of change in these morphological traits.

Larger fin sizes in fish increase maneuverability and stability (Webb 1984), and correspondingly in Atlantic salmon, larger fins occur in populations that occupy faster flowing streams (Riddell and Leggett 1981). Overall, we found that the ray-fins of fish were consistently larger for the $vgll3^{E}$ allele than the $vgll3^{L}$ allele (Supplementary Table 4). However, this improvement for maneuverability and stability may come at the expense of efficiency in longer marine migrations, as a result of increased drag. For example, in coho salmon, juveniles of inland populations with longer migration distances have smaller fins (Taylor and McPhail 1985), which may help reduce drag in long migrations (Dynes *et al.* 2005; Varian and Nichols 2010). A larger cross-section diameter and larger fin lengths associated with the $vgll3^{E}$ allele likely facilitate maneuvering at the expense of efficient cruising, which is in contrast with the $vgll3^{E}$ effect that increases aerobic muscle area and vertebral thickness. Similarly, the slender body (a smaller cross-section diameter) associated with $vgll3^{L}$ is consistent with minimizing drag for a cruising body form (Webb 1988), advantageous for a multi-sea winter strategy that migrates longer distances in the ocean (e.g. O'Sullivan *et al.* 2022). On the other hand, the direction of effect on fin size associated with $vgll3^{E}$ *to* $vgll3^{L}$ substitution is concordant with the effect of the restricted-food regime, suggesting that the allelic substitution effect may be correlated to food limitation conditions. Thus, overall, the direction of *vgll3* genetic effects is not functionally consistent in relation to proposed ecological roles of these morphological traits.

The changes associated with the genetic variation in the *six6* locus that are affecting body and head sizes are linked to ecological processes related to resource acquisition mechanisms. A larger head (and a smaller body) associated with the $six6^{L}$ allele and larger snout length may be associated with a feeding regime toward piscivory (Keeley *et al.* 2005), or generally with consuming larger prey items. This interpretation corroborates the study by Aykanat *et al.* (2020), in which fish with the $six6^{LL}$ genotype were shown to be more efficient in resource acquisition than fish with the $six6^{EE}$ genotype.

Evolvabilities (I_A) ranged from normal to very high compared with a recent meta-analysis (Hansen *et al.* 2011). The median evolvability for length traits is 0.001 (or 0.1%, Hansen and Pélabon 2021; Hansen *et al.* 2011). Normal evolvability values were found for centroid sizes and cross-section diameters, while aerobic muscle and vertebrae thickness had high evolvabilities, suggesting that these traits could evolve rapidly in response to selection induced by environmental change. Interestingly, a substantial portion of the additive genetic variation associated with some traits, such as aerobic muscle area and vertebrae thickness, was explained by the *vgll3* locus, suggesting the locus' importance in shaping the additive genetic landscape.

Taken together, *vgll3* and *six6* loci have complex associations with morphology. These do not consistently align with adaptive differences between early- and late-maturation genotypes associated with marine migration, but could be important at other life stages e.g. during spawning where higher maneuverability of smaller males may be beneficial for reproductive success, or in early life. On the other hand, it is also plausible that these changes are genetically correlated as part of broad development changes, and some of which may have potentially maladaptive consequences. When traits are genetically correlated, the cumulative adaptive value of trait values cannot be optimal (Schluter 1996), since breaking suboptimal trait combinations that are genetically correlated may be challenging during the course of evolution (Blows 2007). Finally, it is challenging to assess the biological significance of the scale of trait variation between loci. However, effect size appears to be large for some trait, i.e. as inferred by up to 50% effect size of allelic substitution effect relative to the effect of length (Supplementary Fig. 4), indicating that the genetic variation produces some static allometry between individuals the same cohort, which may have functional and adaptive basis (Pelabon *et al.* 2014).

It is important to recognize that extrapolation to the marine stage of Atlantic salmon based on juvenile morphology may have limitations. It is unknown if the genotype-associated morphological variation is correlated between juvenile and adult stages. While there may be genetic correlation between freshwater and marine environments (Taylor and McPhail 1985; Fleming *et al.* 1994 ; Morinville and Rasmussen 2006), the morphological changes associated with adaptation to the marine environment, i.e. the parr-smolt transformation (smoltification), may break apart trait correlations, similar to how metamorphosis takes place in many animal taxa (e.g. Aguirre *et al.* 2014). Since the data in this study were composed of individuals that had completed the parr-smolt transformation, or are close to completion, conclusions are likely more relevant to marine stages than the freshwater stages. However, any adaptive inference associated with a specific life stage should be taken with caution until observed patterns are further tested and verified at different life stages. Finally, while it is reasonable to hypothesize that the observed *vgll3* and *six6* associated morphological variation is adaptively important, the fitness effects of this variation should be better assessed before any evolutionary conclusions can be made (Kingsolver *et al.* 1995).

While modeling non-additive architecture within a locus, such as dominance, overdominance, may be relevant, since the *vgll3* locus exhibits sex-dependent dominance (Barson *et al.* 2015), in this study, genetic effects were modeled additively, to avoid conceptual and statistical complexities. However, when genetic effects were modeled non-additively (separately for *vgll3* and *six6*), parsimony was meaningfully improved (i.e. AIC for dominance gene effect model was 2 units smaller than the AIC for additive gene effect model) for 4 out of 21 traits for the *vgll3* gene, while none of the non-additive models performed better than additive models for the *six6* gene (Supplementary Fig. 6a). In all 3 traits with significant non-additive genetic effect, a dominance model with $vgll3^{EL}$ effect resembling $vgll3^{LL}$ was supported (Supplementary Fig. 6b–d), suggesting a possible role of dominance shaping some of the trait values.

In conclusion, we have detected substantial morphological variation associated with 2 genomic regions, which are also major determinants of life-history variation and known to be under local selection. These loci appear to influence multiple, strongly correlated traits, suggestive of a broad regulatory role with impacts

Downloaded from https://academic.oup.com/g3journal/article/15/7/jkaf106/8142704 by Finnish Forest Research Institute / Library user on 16 December 2025

across the whole life cycle. How these genetic correlations are shaped—via single locus pleiotropy or close physical linkage of multiple genes—remains to be determined.

Data availability

The compiled data and R codes to reproduce the results are available in Figshare at https://doi.org/10.6084/m9.figshare.27930231.v1.

Supplemental material available at G3 online.

Acknowledgments

We thank Artur Porto for discussion related to morphometric analyses, and Seija Tillanen, Jacqueline E. Moustakas-Verho, Nikolai Piavchenko for helps with the sampling. Open access funded by Helsinki University Library.

Funding

This work was supported by the Research Council of Finland (grant nos. 328860, 353388, and 325964 to TA, and 314254, 327255 and 342851 to CRP), and the European Research Council under the European Articles Union's Horizon 2020 and Horizon Europe research and innovation programs (grant no. 742312 and 101054307 to CRP). Views and opinions expressed are however those of the author(s) only and do not necessarily reflect those of the European Union or the European Research Council Executive Agency. Neither the European Union nor the granting authority can be held responsible for them. LG was supported by Erasmus + programme.

Conflicts of interest

The author(s) declare no conflict of interest.

Author contributions

TA, VLP, and GHB conceptualized the paper. TA analyzed the data with significant input from GHB and PVD. SJ and LG performed landmarking. AHH and AR prepared and scanned the cross-sections. JE, and CRP oversaw the resources and infrastructure. PVD and CRP devised the breeding design and reared the fish. TA and PVD sampled the fish and digitized the images. TA drafted the MS with significant inputs from PVD, VLP, and GHB, and all co-authors contributed to subsequent drafts.

Ethical approval

The experiments were approved by the Project Authorization Board on behalf of the Regional Administrative Agency for Southern Finland (ESAVI) under experimental license ESAVI/2778/2018.

Literature cited

Aguirre JD, Blows MW, Marshall DJ. 2014. The genetic covariance between life cycle stages separated by metamorphosis. Proc Biol Sci. 281(1788):20141091. doi:10.1098/rspb.2014.1091.

Ahi EP, Sinclair-Waters M, Moustakas-Verho J, Jansouz S, Primmer CR. 2022. Strong regulatory effects of vgll3 genotype on reproductive axis gene expression in juvenile male Atlantic salmon. Gen Comp Endocrinol. 325:114055. doi:10.1016/j.ygcen.2022.114055.

Altringham JD, Ellerby DJ. 1999. Fish swimming: patterns in muscle function. J Exp Biol. 202(23):3397–3403. doi:10.1242/jeb.202.23.3397.

Archambeault SL, Bartschi LR, Merminod AD, Peichel CL. 2020. Adaptation via pleiotropy and linkage: association mapping reveals a complex genetic architecture within the stickleback Eda locus. Evol Lett. 4(4):282–301. doi:10.1002/evl3.175.

Asheim ER, Debes PV, House A, Liljestrom P, Niemela PT, Siren JP, Erkinaro J, Primmer CR. 2023. Atlantic salmon (*Salmo salar*) age at maturity is strongly affected by temperature, population and age-at-maturity genotype. Conserv Physiol. 11(1):coac086. doi:10.1093/conphys/coac086.

Aykanat T, McLennan D, Metcalfe NB, Prokkola JM. 2024. Early survival in Atlantic salmon is associated with parental genotypes at loci linked to timing of maturation. Evolution. 78(8):1441–1452. doi:10.1093/evolut/qpae072.

Aykanat T, Ozerov M, Vaha JP, Orell P, Niemela E, Erkinaro J, Primmer CR. 2019. Co-inheritance of sea age at maturity and iteroparity in the Atlantic salmon vgll3 genomic region. J Evol Biol. 32(4):343–355. doi:10.1111/jeb.13418.

Aykanat T, Rasmussen M, Ozerov M, Niemela E, Paulin L, Vaha J-P, Hindar K, Wennevik V, Pedersen T, Svenning M-A, *et al.* 2020. Life-history genomic regions explain differences in Atlantic salmon marine diet specialization. J Anim Ecol. 89(11):2677–2691. doi:10.1111/1365-2656.13324.

Ayllon F, Kjaerner-Semb E, Furmanek T, Wennevik V, Solberg MF, Dahle G, Taranger GL, Glover KA, Almén MS, Rubin CJ, *et al.* 2015. The vgll3 locus controls age at maturity in wild and domesticated Atlantic salmon (*Salmo salar* L.) males. PLoS Genet. 11(11):e1005628. doi:10.1371/journal.pgen.1005628.

Baken EK, Collyer ML, Kaliontzopoulou A, Adams DC. 2021. Geomorph v4.0 and gmShiny: enhanced analytics and a new graphical interface for a comprehensive morphometric experience. Methods Ecol Evol. 12(12):2355–2363. doi:10.1111/2041-210x.13723.

Bangura PB, Tiira K, Niemela PT, Erkinaro J, Liljestrom P, Toikkanen A, Primmer CR. 2022. Linking vgll3 genotype and aggressive behaviour in juvenile Atlantic salmon (*Salmo salar*). J Fish Biol. 100(5):1264–1271. doi:10.1111/jfb.15040.

Barrett RD, Hoekstra HE. 2011. Molecular spandrels: tests of adaptation at the genetic level. Nat Rev Genet. 12(11):767–780. doi:10.1038/nrg3015.

Barson NJ, Aykanat T, Hindar K, Baranski M, Bolstad GH, Fiske P, Jacq C, Jensen AJ, Johnston SE, Karlsson S, *et al.* 2015. Sex-dependent dominance at a single locus maintains variation in age at maturity in salmon. Nature. 528(7582):405–408. doi:10.1038/nature16062.

Bates D, Mächler M, Bolker B, Walker S. 2015. Fitting linear mixed-effects models using lme4. J Stat Softw. 67(1):1–48. doi:10.18637/jss.v067.i01.

Baxter D, Cohen KE, Donatelli CM, Tytell ED. 2022. Internal vertebral morphology of bony fishes matches the mechanical demands of different environments. Ecol Evol. 12(11):e9499. doi:10.1002/ece3.9499.

Blows MW. 2007. A tale of two matrices: multivariate approaches in evolutionary biology. J Evol Biol. 20(1):1–8. doi:10.1111/j.1420-9101.2006.01164.x.

Boyle EA, Li YI, Pritchard JK. 2017. An expanded view of complex traits: from polygenic to omnigenic. Cell. 169(7):1177–1186. doi:10.1016/j.cell.2017.05.038.

Chan YF, Marks ME, Jones FC, Villarreal G Jr, Shapiro MD, Brady SD, Southwick AM, Absher DM, Grimwood J, Schmutz J, *et al.* 2010. Adaptive evolution of pelvic reduction in sticklebacks by

Downloaded from https://academic.oup.com/g3journal/article/15/7/jkaf106/8142704 by Finnish Forest Research Institute / Library user on 16 December 2025

recurrent deletion of a Pitx1 enhancer. Science. 327(5963): 302–305. doi:10.1126/science.1182213.

Collyer ML, Adams DC, Freckleton R. 2018. RRPP: an R package for fitting linear models to high-dimensional data using residual randomization. Methods Ecol Evol. 9(7):1772–1779. doi:10.1111/2041-210x.13029.

Colosimo PF, Hosemann KE, Balabhadra S, Villarreal G Jr, Dickson M, Grimwood J, Schmutz J, Myers RM, Schluter D, Kingsley DM. 2005. Widespread parallel evolution in sticklebacks by repeated fixation of Ectodysplasin alleles. Science. 307(5717):1928–1933. doi:10.1126/science.1107239.

Crossin GT, Hinch SG, Farrell AP, Higgs DA, Lotto AG, Oakes JD, Healey MC. 2004. Energetics and morphology of sockeye salmon: effects of upriver migratory distance and elevation. J Fish Biol. 65(3):788–810. doi:10.1111/j.0022-1112.2004.00486.x.

Debes PV, Piavchenko N, Erkinaro J, Primmer CR. 2020. Genetic growth potential, rather than phenotypic size, predicts migration phenotype in Atlantic salmon. Proc Biol Sci. 287(1931):20200867. doi:10.1098/rspb.2020.0867.

Debes PV, Piavchenko N, Ruokolainen A, Ovaskainen O, Moustakas-Verho JE, Parre N, Aykanat T, Erkinaro J, Primmer CR. 2019. Large single-locus effects for maturation timing are mediated via condition variation in Atlantic salmon . bioRxiv 780437. https://doi.org/10.1101/780437, preprint: not peer reviewed.

Debes PV, Piavchenko N, Ruokolainen A, Ovaskainen O, Moustakas-Verho JE, Parre N, Aykanat T, Erkinaro J, Primmer CR. 2021. Polygenic and major-locus contributions to sexual maturation timing in Atlantic salmon. Mol Ecol. 30(18):4505–4519. doi:10.1111/mec.16062.

Donatelli CM, Roberts AS, Scott E, DeSmith K, Summers D, Abu-Bader L, Baxter D, Standen EM, Porter ME, Summers AP, *et al.* 2021. Foretelling the flex-vertebral shape predicts behavior and ecology of fishes. Integr Comp Biol. 61(2):414–426. doi:10.1093/icb/icab110.

Dynes J, Magnan P, Bernatchez L, Rodríguez MA. 2005. Genetic and morphological variation between two forms of lacustrine brook charr. J Fish Biol. 54(5):955–972. doi:10.1111/j.1095-8649.1999.tb00850.x.

Eliason EJ, Farrell AP. 2015. Oxygen uptake in Pacific salmon *Oncorhynchus* spp.: when ecology and physiology meet. J Fish Biol. 88(1):359–388. doi:10.1111/jfb.12790.

Elmer KR, Kusche H, Lehtonen TK, Meyer A. 2010. Local variation and parallel evolution: morphological and genetic diversity across a species complex of neotropical crater lake cichlid fishes. Philos Trans R Soc Lond B Biol Sci. 365(1547):1763–1782. doi:10.1098/rstb.2009.0271.

Endler JA. 2000. Adaptive genetic variation in the wild. In: Mousseau TA, SinerVo B, Endler JA, editors. Adaptive Genetic Variation in the Wild. New York: Oxford University Press. p. 251–260.

Ferry-Graham LA, Bolnick DI, Wainwright PC. 2002. Using functional morphology to examine the ecology and evolution of specialization. Integr Comp Biol. 42(2):265–277. doi:10.1093/icb/42.2.265.

Fitzgerald DB, Winemiller KO, Sabaj Pérez MH, Sousa LM, Seymour C. 2017. Using trophic structure to reveal patterns of trait-based community assembly across niche dimensions. Funct Ecol. 31(5):1135–1144. doi:10.1111/1365-2435.12838.

Fleming IA, Jonsson B, Gross MR. 1994. Phenotypic divergence of sea-ranched, farmed, and wild salmon. Can J Fish Aquat Sci. 51(12):2808–2824. doi:10.1139/f94-280.

Gelman A, Su YS. 2020. arm: Data analysis using regression and multilevel/hierarchical models. R package version 1.11-2.

Gower JC. 1975. Generalized procrustes analysis. Psychometrika. 40(1):33–51. doi:10.1007/bf02291478.

Hansen TF, Pélabon C. 2021. Evolvability: a quantitative-genetics perspective. Annu Rev Ecol Evol Syst. 52(1):153–175. doi:10.1146/annurev-ecolsys-011121-021241.

Hansen TF, Pelabon C, Armbruster WS, Carlson ML. 2003. Evolvability and genetic constraint in *Dalechampia* blossoms: components of variance and measures of evolvability. J Evol Biol. 16(4):754–766. doi:10.1046/j.1420-9101.2003.00556.x.

Hansen TF, Pélabon C, Houle D. 2011. Heritability is not evolvability. Evol Biol. 38(3):258–277. doi:10.1007/s11692-011-9127-6.

Hoar WS. 1988. The physiology of smolting salmonids. In: Hoar WS, Randall DJ, editors. Fish Physiology. San Diego: Academic Press. Vol. 11. p. 275–343.

Houle D. 1992. Comparing evolvability and variability of quantitative traits. Genetics. 130(1):195–204. doi:10.1093/genetics/130.1.195.

Huang J, Wu S, Barrera J, Matthews K, Pan D. 2005. The Hippo signaling pathway coordinately regulates cell proliferation and apoptosis by inactivating Yorkie, the *Drosophila* homolog of YAP. Cell. 122(3):421–434. doi:10.1016/j.cell.2005.06.007.

Jakobson CM, Jarosz DF. 2020. What has a century of quantitative genetics taught US about nature's genetic tool kit? Annu Rev Genet. 54(1):439–464. doi:10.1146/annurev-genet-021920-102037.

Jimenez-Gomez JM, Wallace AD, Maloof JN. 2010. Network analysis identifies ELF3 as a QTL for the shade avoidance response in *Arabidopsis*. PLoS Genet. 6(9):e1001100. doi:10.1371/journal.pgen.1001100.

Jones FC, Grabherr MG, Chan YF, Russell P, Mauceli E, Johnson J, Swofford R, Pirun M, Zody MC, White S, *et al.* 2012. The genomic basis of adaptive evolution in threespine sticklebacks. Nature. 484(7392):55–61. doi:10.1038/nature10944.

Jonsson B, Jonsson N. 2011. Ecology of Atlantic salmon and Brown Trout: Habitat as a Template for Life Histories. Dordrecht.: Springer.

Kawecki TJ, Ebert D. 2004. Conceptual issues in local adaptation. Ecol Lett. 7(12):1225–1241. doi:10.1111/j.1461-0248.2004.00684.x.

Keeley ER, Parkinson EA, Taylor EB. 2005. Ecotypic differentiation of native rainbow trout (*Oncorhynchus mykiss*) populations from British Columbia. Can J Fish Aquat Sci. 62(7):1523–1539. doi:10.1139/f05-062.

Kern EMA, Robinson D, Gass E, Godwin J, Langerhans RB. 2016. Correlated evolution of personality, morphology and performance. Anim Behav. 117:79–86. doi:10.1016/j.anbehav.2016.04.007.

King DE. 2009. Dlib-Ml: a machine learning toolkit. J Mach Learn Res. 10:1755–1758. doi:10.1145/1577069.1755843.

Kingsolver JG, Woods HA, Gilchrist G. 1995. Traits related to fitness. Science. 267(5196):396. doi:10.1126/science.267.5196.396.

Klingenberg CP. 2016. Size, shape, and form: concepts of allometry in geometric morphometrics. Dev Genes Evol. 226(3):113–137. doi:10.1007/s00427-016-0539-2.

Kurko J, Debes PV, House AH, Aykanat T, Erkinaro J, Primmer CR. 2020. Transcription profiles of age-at-maturity-associated genes suggest cell fate commitment regulation as a key factor in the Atlantic salmon maturation process. G3 (Bethesda). 10(1): 235–246. doi:10.1534/g3.119.400882.

Kuznetsova A, Brockhoff PB, Christensen RHB. 2017. lmerTest package: tests in linear mixed effects models. J Stat Softw. 82(13):1–26. doi:10.18637/jss.v082.i13.

Long JH, Nipper KS. 1996. The importance of body stiffness in undulatory propulsion. Am Zool. 36(6):678–694. doi:10.1093/icb/36.6.678.

Lundsgaard-Hansen B, Matthews B, Vonlanthen P, Taverna A, Seehausen O. 2013. Adaptive plasticity and genetic divergence in feeding efficiency during parallel adaptive radiation of whitefish (*Coregonus* spp.). J Evol Biol. 26(3):483–498. doi:10.1111/jeb.12063.

Downloaded from https://academic.oup.com/g3journal/article/15/7/jkaf106/8142704 by Finnish Forest Research Institute / Library user on 16 December 2025

Luo L, Mao Y, Xu S. 2003. Correcting the bias in estimation of genetic variances contributed by individual QTL. Genetica. 119(2): 107–113. doi:10.1023/a:1026028928003.

Lynch M, Walsh B. 1998. Genetics and Analysis of Quantitative Traits. Sunderland (MA): Sinauer Associates.

Mackay TF, Stone EA, Ayroles JF. 2009. The genetics of quantitative traits: challenges and prospects. Nat Rev Genet. 10(8):565–577. doi:10.1038/nrg2612.

Miettinen A, Dannewitz J, Palm S, Ahi EP, Romakkaniemi A, Vähä V, Östergren J, Primmer CR, Pritchard VL. 2023. Loci associated with maturation, migration and appetite control are linked with signals of fine-scale local selection in a large Atlantic salmon population. bioRxiv 553800. https://doi.org/10.1101/2023.08.23.553800, preprint: not peer reviewed.

Mindel BL, Neat FC, Trueman CN, Webb TJ, Blanchard JL. 2016. Functional, size and taxonomic diversity of fish along a depth gradient in the deep sea. PeerJ. 4:e2387. doi:10.7717/peerj.2387.

Mobley KB, Aykanat T, Czorlich Y, House A, Kurko J, Miettinen A, Moustakas-Verho J, Salgado A, Sinclair-Waters M, Verta J-P, *et al.* 2021. Maturation in Atlantic salmon (*Salmo salar*, Salmonidae): a synthesis of ecological, genetic, and molecular processes. Rev Fish Biol Fish. 31(3):523–571. doi:10.1007/s11160-021-09656-w.

Morinville GR, Rasmussen JB. 2006. Does life-history variability in salmonids affect habitat use by juveniles? A comparison among streams open and closed to anadromy. J Anim Ecol. 75(3): 693–704. doi:10.1111/j.1365-2656.2006.01090.x.

Morinville GR, Rasmussen JB. 2007. Distinguishing between juvenile anadromous and resident brook trout (*Salvelinus fontinalis*) using morphology. Environ Biol Fishes. 81(2):171–184. doi:10.1007/s10641-007-9186-9.

Moustakas-Verho JE, Kurko J, House AH, Erkinaro J, Debes P, Primmer CR. 2020. Developmental expression patterns of six6: a gene linked with spawning ecotypes in Atlantic salmon. Gene Expr Patterns. 38:119149. doi:10.1016/j.gep.2020.119149.

Nielsen EE, Hemmer-Hansen J, Larsen PF, Bekkevold D. 2009. Population genomics of marine fishes: identifying adaptive variation in space and time. Mol Ecol. 18(15):3128–3150. doi:10.1111/j.1365-294X.2009.04272.x.

Olson-Manning CF, Wagner MR, Mitchell-Olds T. 2012. Adaptive evolution: evaluating empirical support for theoretical predictions. Nat Rev Genet. 13(12):867–877. doi:10.1038/nrg3322.

Orr HA. 2000. Adaptation and the cost of complexity. Evolution. 54(1):13–20. doi:10.1111/j.0014-3820.2000.tb00002.x.

O'Sullivan RJ, Ozerov M, Bolstad GH, Gilbey J, Jacobsen JA, Erkinaro J, Rikardsen AH, Hindar K, Aykanat T. 2022. Genetic stock identification reveals greater use of an oceanic feeding ground around the Faroe Islands by multi-sea winter Atlantic salmon, with variation in use across reporting groups. ICES J Mar Sci. 79(9): 2442–2452. doi:10.1093/icesjms/fsac182.

Otto SP. 2004. Two steps forward, one step back: the pleiotropic effects of favoured alleles. Proc Biol Sci. 271(1540):705–714. doi:10.1098/rspb.2003.2635.

Paaby AB, Rockman MV. 2013. The many faces of pleiotropy. Trends Genet. 29(2):66–73. doi:10.1016/j.tig.2012.10.010.

Pelabon C, Firmat C, Bolstad GH, Voje KL, Houle D, Cassara J, Rouzic AL, Hansen TF. 2014. Evolution of morphological allometry. Ann N Y Acad Sci. 1320(1):58–75. doi:10.1111/nyas.12470.

Peris Tamayo AM, Devineau O, Praebel K, Kahilainen KK, Ostbye K. 2020. A brain and a head for a different habitat: size variation in four morphs of Arctic charr (*Salvelinus alpinus* (L.)) in a deep oligotrophic lake. Ecol Evol. 10(20):11335–11351. doi:10.1002/ece3.6771.

Pritchard VL, Makinen H, Vaha JP, Erkinaro J, Orell P, Primmer CR. 2018. Genomic signatures of fine-scale local selection in Atlantic salmon suggest involvement of sexual maturation, energy homeostasis and immune defence-related genes. Mol Ecol. 27(11):2560–2575. doi:10.1111/mec.14705.

Prokkola JM, Åsheim ER, Morozov S, Bangura P, Erkinaro J, Ruokolainen A, Primmer CR, Aykanat T. 2022. Genetic coupling of life-history and aerobic performance in Atlantic salmon. Proc Biol Sci. 289(1967):20212500. doi:10.1098/rspb.2021.2500.

Proulx R, Magnan P. 2004. Contribution of phenotypic plasticity and heredity to the trophic polymorphism of lacustrine brook charr (*Salvelinus fontinalis* M.). Evol Ecol Res. 6(4):503–522.

R Core Team. 2019. R Foundation for Statistical Computing. Vienna, Austria.

Riddell BE, Leggett WC. 1981. Evidence of an adaptive basis for geographic-variation in body morphology and time of downstream migration of juvenile Atlantic salmon (*Salmo salar*). Can J Fish Aquat Sci. 38(3):308–320. doi:10.1139/f81-042.

Schluter D. 1996. Ecological causes of adaptive radiation. Am Nat. 148:40–64. doi:10.1086/285901.

Shapiro MD, Marks ME, Peichel CL, Blackman BK, Nereng KS, Jonsson B, Schluter D, Kingsley DM. 2004. Genetic and developmental basis of evolutionary pelvic reduction in threespine sticklebacks. Nature. 428(6984):717–723. doi:10.1038/nature02415.

Shuman JL, Coughlin DJ. 2018. Red muscle function and thermal acclimation to cold in rainbow smelt, *Osmerus mordax*, and rainbow trout, *Oncorhynchus mykiss*. J Exp Zool A Ecol Integr Physiol. 329(10):547–556. doi:10.1002/jez.2219.

Simonsen MK, Siwertsson A, Adams CE, Amundsen PA, Praebel K, Knudsen R. 2017. Allometric trajectories of body and head morphology in three sympatric Arctic charr (*Salvelinus alpinus* (L.)) morphs. Ecol Evol. 7(18):7277–7289. doi:10.1002/ece3.3224.

Sinclair-Waters M, Ødegård J, Korsvoll SA, Moen T, Lien S, Primmer CR, Barson NJ. 2020. Beyond large-effect loci: large-scale GWAS reveals a mixed large-effect and polygenic architecture for age at maturity of Atlantic salmon. Genet Sel Evol. 52(1):9. doi:10.1186/s12711-020-0529-8.

Snorrason S. 1994. Trophic specialization in Arctic charr *Salvelinus alpinus* (Pisces; Salmonidae): morphological divergence and ontogenetic niche shifts. Biol J Linn Soc. 52(1):1–18. doi:10.1006/bijl.1994.1035.

Solovieff N, Cotsapas C, Lee PH, Purcell SM, Smoller JW. 2013. Pleiotropy in complex traits: challenges and strategies. Nat Rev Genet. 14(7):483–495. doi:10.1038/nrg3461.

Svanbäck R, Eklöv P. 2003. Morphology dependent foraging efficiency in perch: a trade-off for ecological specialization? Oikos. 102(2): 273–284. doi:10.1034/j.1600-0706.2003.12657.x.

Takacs P, Vital Z, Ferincz Á, Staszny Á. 2016. Repeatability, reproducibility, separative power and subjectivity of different fish morphometric analysis methods. PLoS One. 11(6):e0157890. doi:10.1371/journal.pone.0157890.

Taylor EB, McPhail JD. 1985. Variation in body morphology among British Columbia populations of coho salmon, *Oncorhynchus kisutch*. Can J Fish Aquat Sci. 42(12):2020–2028. doi:10.1139/f85-249.

Varian A, Nichols KM. 2010. Heritability of morphology in brook trout with variable life histories. PLoS One. 5(9):e12950. doi:10.1371/journal.pone.0012950.

Vazquez AI, Bates DM, Rosa GJ, Gianola D, Weigel KA. 2010. Technical note: an R package for fitting generalized linear mixed models in animal breeding. J Anim Sci. 88(2):497–504. doi:10.2527/jas.2009-1952.

Downloaded from https://academic.oup.com/g3journal/article/15/7/jkaf106/8142704 by Finnish Forest Research Institute / Library user on 16 December 2025

Verta J-P, Debes PV, Piavchenko N, Ruokolainen A, Ovaskainen O, Moustakas-Verho JE, Tillanen S, Parre N, Aykanat T, Erkinaro J, *et al.* 2020. Cis-regulatory differences in isoform expression associate with life history strategy variation in Atlantic salmon. PLoS Genet. 16(9):e1009055. doi:10.1371/journal.pgen.1009055.

Verta J-P, Moustakas-Verho JE, Donner I, Frapin M, Ruokolainen A, Debes PV, Erkinaro J, Primmer CR. 2024. A complex mechanism translating variation of a simple genetic architecture into alternative life histories. Proc Natl Acad Sci U S A. 121(48): e2402386121. doi:10.1073/pnas.2402386121.

Vrdoljak J, Sanchez KI, Arreola-Ramos R, Diaz Huesa EG, Villagra A, Avila LJ, Morando M. 2020. Testing repeatability, measurement error and species differentiation when using geometric morphometrics on complex shapes: a case study of Patagonian lizards of the genus *Liolaemus* (Squamata: Liolaemini). Biol J Linn Soc. 130(4):800–812. doi:10.1093/biolinnean/blaa079.

Wagner GP, Altenberg L. 1996. Perspective: complex adaptations and the evolution of evolvability. Evolution. 50(3):967–976. doi:10.1111/j.1558-5646.1996.tb02339.x.

Wagner GP, Zhang J. 2011. The pleiotropic structure of the genotype-phenotype map: the evolvability of complex organisms. Nat Rev Genet. 12(3):204–213. doi:10.1038/nrg2949.

Webb PW. 1984. Body form, locomotion and foraging in aquatic vertebrates. Am Zool. 24(1):107–120. doi:10.1093/icb/24.1.107.

Webb PW. 1988. Simple physical principles and vertebrate aquatic locomotion. Am Zool. 28(2):709–725. doi:10.1093/icb/28.2.709.

Weith M, Grossbach J, Clement-Ziza M, Gillet L, Rodriguez-Lopez M, Marguerat S, Workman CT, Picotti P, Bähler J, Aebersold R, *et al.* 2023. Genetic effects on molecular network states explain complex traits. Mol Syst Biol. 19(8):e11493. doi:10.15252/msb.202211493.

Wu MY, Hill CS. 2009. TGF-beta superfamily signaling in embryonic development and homeostasis. Dev Cell. 16(3):329–343. doi:10.1016/j.devcel.2009.02.012.

Xue C, Chu Q, Shi Q, Zeng Y, Lu J, Li L. 2025. Wnt signaling pathways in biology and disease: mechanisms and therapeutic advances. Signal Transduct Target Ther. 10(1):106. doi:10.1038/s41392-025-02142-w.

Ziyatdinov A, Vazquez-Santiago M, Brunel H, Martinez-Perez A, Aschard H, Soria JM. 2018. Lme4qtl: linear mixed models with flexible covariance structure for genetic studies of related individuals. BMC Bioinformatics. 19(1):68. doi:10.1186/s12859-018-2057-x.

Zueva KJ, Lumme J, Veselov AE, Primmer CR, Pritchard VL. 2020. Population genomics reveals repeated signals of adaptive divergence in the Atlantic salmon of north-eastern Europe. J Evol Biol. 34(6):866–878. doi:10.1111/jeb.13732.

Editor: D.-J. de Koning

Downloaded from https://academic.oup.com/g3journal/article/15/7/jkaf106/8142704 by Finnish Forest Research Institute / Library user on 16 December 2025